Structure of a Liquid Crystalline Metallosupramolecular Polyelectrolyte–Amphiphile Complex at the Nanoscopic Level

ARTICLE *in* LANGMUIR · MAY 2003

Impact Factor: 4.46 · DOI: 10.1021/la026757g · Source: OAI

4 AUTHORS, INCLUDING:

Andreas F Thünemann

Bundesanstalt für Materialforschung und -pr…

178 PUBLICATIONS **4,958** CITATIONS

Structure of a Liquid Crystalline Metallosupramolecular Polyelectrolyte−Amphiphile Complex at the Nanoscopic Level

Dirk G. Kurth,*,† Annette Meister,† Andreas F. Thünemann,‡ and Günter Förster§

Max Planck Institute of Colloids and Interfaces, D-14476 Golm, Germany, Fraunhofer Institute for Applied Polymer Research, D-14476 Golm, Germany, and Martin Luther University Halle-Wittenberg, Institute of Physical Chemistry, D-06099 Halle, Germany

Received October 26, 2002

The solid-state organization of a liquid crystalline metallosupramolecular polyelectrolyte−amphiphile complex at the nanoscopic level is decoded by a combination of X-ray scattering and molecular modeling. The nanostructured material, which self-assembles from transition metal ions, ditopic ligands, and amphiphiles, has a hierarchical architecture consisting of alternating strata of metallo units and interdigitated amphiphiles.

Introduction

Amphiphilic self-assembly is by far the most fundamental mechanism for the construction of soft matter materials.[1] Amphiphilic molecules can adapt a multitude of hierarchical architectures with distinct geometries including bilayers and spherical and cylindrical micelles arranged in cubic, hexagonal, or lamellar superstructures. The interaction of amphiphiles and charged macromolecules can result in new soft condensed phases exhibiting complex polymorphism and novel properties.[2,3] These materials have significant technological value for applications such as lubricants,[4] cosmetics,[5] and gene therapeutics.[6]

In addition, amphiphilic self-assembly offers a promising solution to a prevailing problem in supramolecular materials chemistry. The ability to control the spatial arrangement of functional constituents is of critical importance with respect to the encoding of new (collective) properties and the full exploitation of a material's potential. The combination of supramolecular modules (SUMOs) as functional and amphiphiles as structural components appears as an attractive route toward this goal. While metallomesogens have been known for a long time, the combination of SUMOs and amphiphiles has hardly been researched systematically.[7]

Metallosupramolecular modules (MEMOs) originating from metal-ion-directed self-assembly are of particular interest for the construction of functional devices because they possess diverse structural, functional, reactive, thermodynamic, and kinetic properties.[8−10] Due to the numerous properties of MEMOs, one can envision a wide variety of applications that utilize photons, electrons, and spin transitions.[11] With the recent discovery of metallosupramolecular coordination polyelectrolytes (MEPEs), novel components are now available that facilitate the entry into metallofunctionalized polyelectrolyte−amphiphile complexes (PACs).[12] Here, we present the first account of such a PAC architecture. The absence of symmetrical invariance (e.g., crystallinity) in such materials represents a central challenge in structural characterization,[13] and therefore, we describe an attempt to apply a combination of X-ray analysis and molecular mechanics modeling to reveal structural details down to the nanoscopic level.

Experimental Section

Materials. The MEPE and PAC were synthesized according to previously published procedures.[12,22]

Measurements. Differential scanning calorimetry (DSC) measurements were performed on a Netsch DSC 200 (Germany). The samples were examined at a scanning rate of 10 K/min by applying one cooling and two heating scans. The X-ray scattering measurements were recorded with an X-ray vacuum camera with pinhole collimation (Anton Paar, Austria; model A-8054) equipped with image plates (type BAS III, Fuji, Japan). The image plates were read by a MACScience Dip-Scanner IPR-420 and IP reader DIPR-420 (Japan). The scattering vector s is defined as $s = 2/\lambda \sin\theta$, where 2θ is the angle between the primary and the scattered beam and λ is the wavelength (Cu Kα). The PAC films had a thickness of 0.01−0.1 mm.

Modeling. Modeling, static lattice energy minimizations, and simulations of X-ray scattering patterns were performed using the Cerius^2 software, release 4.2 (Accelrys Inc.), on a workstation Octane2 under Irix, release 6.5 (Silicon Graphics Inc.). The Universal force field was chosen because it can handle both metal ion complexes and amphiphilic molecules. Charges were calculated with the charge equilibration method. The Ewald sum method was used for the lattice energy minimization.

Results and Discussion

As shown in Scheme 1, PAC **1** is prepared by sequential self-assembly of 1,4-bis(2,2′:6′,2″-terpyridine-4′-yl)ben-

† Max Planck Institute of Colloids and Interfaces.

‡ Fraunhofer Institute for Applied Polymer Research.

§ Martin Luther University Halle-Wittenberg.

(1) Tomalia, D. A.; Wang, Z.-G.; Tirrell, M. *Curr. Opin. Colloid Interface Sci.* **1999**, *4*, 3−5.

(2) Ober, C. K.; Wegner, G. *Adv. Mater.* **1997**, *9*, 17−31.

(3) Kosmella, S.; Kotz, J.; Shirahama, K.; Liu, J. *J. Phys. Chem. B* **1998**, *102*, 6459−6464.

(4) Thünemann, A. F. *Polym. Int.* **2000**, *49*, 636−644.

(5) Andre, V.; Norenberg, R.; Hossel, P.; Pfau, A. *Macromol. Symp.* **1999**, *145*, 169−179.

(6) Brown, M. D.; Schätzlein, A. G.; Uchegbu, I. F. *Int. J. Pharm.* **2001**, *229*, 1−21.

(7) Giroud-Godquin, A. M. *Coord. Chem. Rev.* **1998**, *178−180*, 1485−1499.

(8) Lehn, J.-M. *Supramolecular Chemistry − Concepts and Perspectives*; VCH: Weinheim, 1995.

(9) Holliday, B. J.; Mirkin, C. A. *Angew. Chem.* **2001**, *113*, 2076−2098; *Angew. Chem., Int. Ed.* **2001**, *40*, 2022−2043.

(10) Muchado, V. G.; Baxter, P. N. W.; Lehn, J.-M. *J. Braz. Chem. Soc.* **2001**, *12*, 431−461.

(11) Kurth, D. G. *Ann. N.Y. Acad. Sci.* **2002**, *960*, 29−39.

(12) Schütte, M.; Kurth, D. G.; Linford, M. R.; Cölfen H.; Möhwald, H. *Angew. Chem.* **1998**, *110*, 3058−3061; *Angew. Chem., Int. Ed.* **1998**, *37*, 2891−2893.

(13) Antonietti, M.; Burger, C.; Thünemann, A. *Trends Polym. Sci.* (*Cambridge, U.K.*) **1997**, *5*, 262−267.

10.1021/la026757g CCC: $25.00
Published on Web 01/25/2003

Scheme 1. Self-Assembly of 1,4-Bis(2,2′:6′,2″-terpyridin-4′-yl)benzene, Fe(II), and DHP Results in Two Sequential Steps in PAC[a]

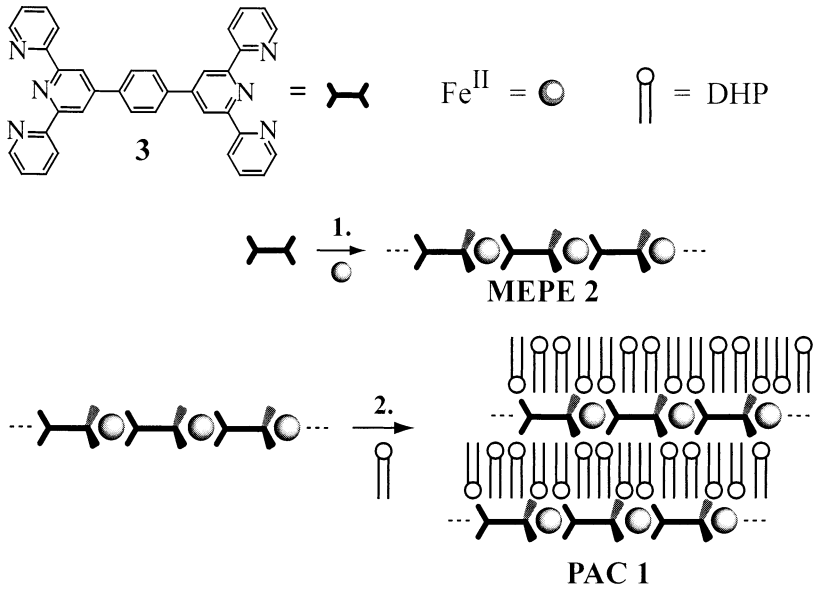

[a] The octahedral coordination geometry is indicated by the wedges. A schematic representation of the lamellar organization of PAC with fully interdigitated DHP molecules and single MEPE strata is shown.

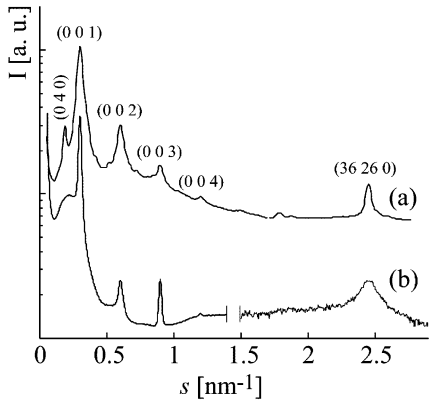

Figure 1. Calculated (a) and experimental (b) X-ray scattering curves of metallosupramolecular PAC **1**.

zene, **3**, with iron acetate followed by assembly with dihexadecyl phosphate (DHP). Complex formation with DHP renders MEPE **2** neutral and hydrophobic, thus effecting transfer into the organic phase. Under the particular assembly conditions, the composition amounts to six DHPs per monomer unit [Fe**3**]$^{2+}$.[14] Presumably, DHP forms a charged hydrogen-bonded network, which binds to MEPE through electrostatic interactions.

The molecular geometry of PAC with a rodlike backbone and mobile amphiphiles suggests liquid crystalline behavior in the solid state. Investigations of the thermal properties by DSC confirm thermotropic polymorphism with two endothermic transitions at 56 and 77 °C. To probe the structure, temperature-dependent small-angle (SAXS) and wide-angle (WAXS) X-ray scattering measurements are carried out on free-standing PAC films. In this article, we will focus on the room-temperature phase. The representative SAXS and WAXS patterns shown in Figure 1 exhibit three sharp scattering peaks with equidistant positions that correspond to a lamellar structure with a translational period of 3.3 nm and a broad peak at smaller values of the scattering vector with a maximum that corresponds to a Bragg distance of about 5 nm. Furthermore, we observe a single peak in the WAXS region that corresponds to a period of 0.41 nm. SAXS and WAXS regions are recorded under different experimental conditions, and therefore, the intensities cannot be compared directly.

We use molecular mechanics modeling to compose the PAC architecture and to refine it at the nanoscopic level until the computed scattering curves best fit the experimental data. We begin the analysis by assuming that PAC forms a flat lamellar phase of alternating stacks of MEPE and DHP. We apply the following conditions to the model: (i) charge balance between both components, (ii) hydrophobic/hydrophilic balance within the amphiphilic layer, and (iii) close space packing. Due to the semiordered nature of the architecture, positional disorder is introduced into the model to suppress the structure factors of crystalline scattering peaks to a value below 0.1% relative intensity.[15]

The starting point of the modeling analysis is the alkyl chain packing mode of the amphiphilic layer.[16] The peak in the WAXS region at a Bragg spacing of 0.41 nm can be assigned to a two-dimensional hexagonal alkyl chain lattice.[17] This is analogous to the hexatic phase of *n*-alkanes.[18] The interlayer spacing of 3.3 nm implies that a single lamella can accommodate only one stratum of DHP molecules because the length of DHP in an all-trans configuration is approximately 2.2 nm.[19] The remaining space is occupied by MEPE, which has an approximate width of 1.15 nm. The DHP stratum consists of interdigitated molecules so that the charged phosphate headgroups, pointing to either side of the stratum, can counterbalance the positive charges of the interstitial MEPE. For the representation of the DHP stratum, we chose an orthorhombic unit cell consisting of 12 DHP molecules, 4 of which are deprotonated, positioned on a

(14) Lehmann, P.; Kurth, D. G.; Brezesinski, G.; Symietz, C. *Chem.—Eur. J.* **2001**, *7*, 1646−1651.

(15) Bernal, J. D.; Crowfoot, D. *Trans. Faraday Soc.* **1933**, *29*, 1032.

(16) Förster, G.; Meister, A.; Blume, A. *Curr. Opin. Colloid Interface Sci.* **2001**, *6*, 294−302.

(17) Thünemann, A. F.; General, S. *Langmuir* **2000**, *16*, 9634−9638.

(18) Seddon, J. M. *Handbook of Liquid Crystals*; Demus, D., Goodby, J., Grey, G. W., Spiess, H.-W., Vill, V., Eds.; Wiley-VCH: Weinheim, 1998; Vol. 1, Chapter 3, p 661.

(19) The infrared spectra of PAC **1** are in agreement with an all-trans configuration of the DHP molecules.

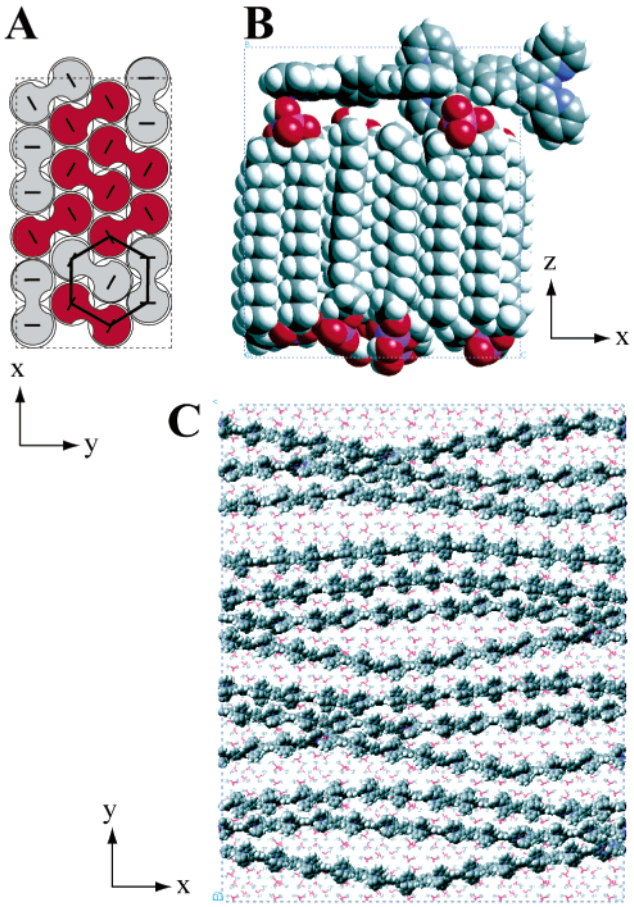

Figure 2. Structural model to compute the scattering pattern of the metallosupramolecular PAC **1**: (A) The hexagonal alkyl chain packing of the orthorhombic DHP unit cell comprising 12 molecules (top view). This unit cell satisfies the steric requirements of the MEPE repeat unit. To preserve electroneutrality, four DHPs are deprotonated. Phosphate groups are randomly oriented toward the top or bottom of the stratum indicated by red or gray coloration (phosphate group not shown for brevity). The small lines indicate the plane of the carbon atoms. (B) The DHP unit cell with randomly oriented headgroups and a MEPE repeat unit (side view). (C) Top view of disordered MEPE chains within a stratum on a layer of DHP.

two-dimensional hexagonal lattice and randomly oriented phosphate headgroups. The area of this unit amounts to approximately 2.4 nm^2 and provides sufficient space to accommodate the MEPE repeat unit ([Fe**3**]$_2$), which occupies an area of approximately 1.8 nm^2.[11] For the energy minimization, we apply the constraint of constant lattice parameters in order to comply with the experimental scattering pattern. Figure 2A schematically depicts the energy-minimized arrangement of the alkyl chains.

Next, the MEPE is assembled and energy minimized. On the basis of the crystal structure of [Fe(terpy)$_2$](ClO$_4$)$_2$, the [Fe**3**]$_2$ repeat unit (see Figure 2B) is constructed, and several repeat units are linked to a polymer chain, which is energy minimized with no further constraints. Finally, a central MEPE repeat unit of the energy-minimized polymer chain is placed in the DHP unit cell such that the long axis is oriented in the *x*-direction of the orthorhombic unit cell (see Figure 2B). The distance between Fe(II) centers and charge-balancing phosphate groups, although oriented randomly within the stratum, is comparable to that of the ions in the single crystal of [Fe(terpy)$_2$](ClO$_4$)$_2$.[20] The assembly is energy minimized with constant lattice parameters in order to conform to the experimental scattering pattern and to prevent disruption of the MEPE chain.

To suppress superfluous peaks in the calculated scattering curves, additional disorder is introduced. Therefore, 78 unit cells are merged and the MEPE rods are randomly rotated and shifted along the long axis. To refine the scattering pattern below 0.2 nm^{-1}, we introduce another length scale in the architecture. We break up the periodicity by randomly spacing the MEPE chains in the stratum. Additionally, we allow the MEPE chains to bend slightly in plane (see Figure 2C). These measures give rise to a scattering peak at very small angles (s < 0.3 nm^{-1}). The broad peak at around s = 0.2 nm^{-1} is, therefore, attributed to a collection of scattering peaks from small domains of (disordered) MEPE chains. The calculated scattering curve of this flat lamellar architecture gives the best fit with the experimental data (see Figure 1). Small deviations in bandwidths and relative intensities are attributed to additional defects and disorder. Further relaxation of periodicity would require even larger unit cells and excessive computer power. Finally, we note that the flat lamella is the most favorable in terms of minimized lattice energy and packing density in comparison to lamellar ribbons and undulated lamellae.[21] This architecture is in marked contrast to that of corresponding Langmuir−Blodgett (LB) multilayers. The LB films also have a lamellar superstructure, but a lamella consists of four strata, namely, DHP, MEPE, MEPE, and DHP.[10a] This comparison demonstrates how the modular nature permits controlling the architecture from molecular to macroscopic length scales.

In conclusion, amphiphilic self-assembly of MEPE and DHP results in a thermotropic soft condensed phase. The hierarchical architecture of PAC consists of flat lamellae of alternating interdigitated DHP and MEPE strata. The diversity of coordination chemistry, the availability of amphiphiles, the ease of formation, and the wide range of possible structures and functions make this approach genuinely interesting.[22,23] Through the judicious choice of amphiphiles, transition metal ions, and ligands, it should be possible to design materials with tailored magneto-, electro-, and/or photochemical properties. In addition, we can anticipate responsive properties because the components are held in place by weak competing interactions. In closing, we note that although X-ray scattering provides only limited structural information about soft materials, the combination with molecular modeling can help to reveal details at all levels of the structural hierarchy because calculated scattering patterns respond remarkably sensitively to modifications at all length scales. The information gained from such analyses may become useful to understand phenomena that involve short-range interactions, such as structural relaxation and ion or electron transport in soft condensed matter.

Acknowledgment. The authors thank Christa Stolle and Helmuth Möhwald. A.M. thanks the French−German Network "Complex fluids: from 3 to 2 dimensions" for financial support. D.G.K. acknowledges financial support through Deutsche Forschungsgemeinschaft (DFG).

LA026757G

(20) Baker, A. T.; Goodwin, H. A. *Aust. J. Chem.* **1985**, *38*, 207−214.

(21) Gallot, B.; Skoulios, A. *Kolloid Z. Z. Polym.* **1966**, *213*, 143−150.

(22) (a) Kurth, D. G.; Lehmann, P.; Schütte, M. *Proc. Natl. Acad. Sci. U.S.A.* **2000**, *97*, 5704−5707. (b) Bruce, D. W. *Inorganic Materials*, 2nd ed.; Bruce, D. W., O'Hare, D., Eds.; Wiley: New York, 1996; Chapter 8.

(23) Oriol, L.; Serrano, J. L. *Adv. Mater.* **1995**, *7*, 348−369.